GUIDEBOOK

The Mid-Triassic Muschelkalk in southern Poland: shallow-marine carbonate sedimentation in a tectonically active basin

Guide to field trip B5 • 26–27 June 2015

Joachim Szulc, Michał Matysik, Hans Hagdorn

31st IAS
Meeting of Sedimentology
Kraków, Poland • June 2015

ORLEN Upstream

www.orlenupstream.pl

DRILLING

RESERVOIR ENGINEERING

E&P PROJECT ANALYSIS

PRODUCTION PROCESSES

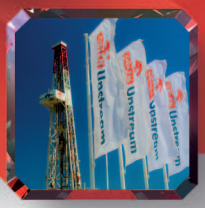

GEOLOGY

GEOPHYSICS

ENVIRONMENTAL PROTECTION HSE

ORLEN GROUP. FUELLING THE FUTURE.

ORLEN Upstream Sp. z o.o.
ul. Prosta 70 | 00-838 Warszawa
Tel.: +48 22 778 02 00 | Fax: +48 22 395 49 69

The Mid-Triassic Muschelkalk in southern Poland: shallow-marine carbonate sedimentation in a tectonically active basin

Joachim Szulc[1], Michał Matysik[2], Hans Hagdorn[3]

[1]Institute of Geological Sciences, Jagiellonian University, Kraków, Poland (joachim.szulc@uj.edu.pl)
[2]Natural History Museum of Denmark, University of Copenhagen, Denmark (ma4tys@interia.pl)
[3]Muschelkalk Musem, Ingelfingen, Germany (encrinus@hagdorn-ingelfingen)

Route (Fig. 1): From Kraków we take motorway A4 west to Chrzanów; we leave it for road 781 to **Płaza** (Kans-Pol quarry, **stop B5.1**). From Płaza we return to A4, continue west to Mysłowice and leave for road A1 to **Siewierz** (GZD **quarry**, **stop B5.2**). From Siewierz we drive A1 south to Podskale cross where we leave for S1 westbound to Pyrzowice and then by road 78 to Niezdara. Then we take road 912 northward to Żyglin (**Żyglin quarry**, **stop B5.3**). From Żyglin we drive by road 908 to Tarnowskie Góry then to NW by road 11 to Tworog. From Tworog west by road 907 to Toszek and then west by road 94 to Strzelce Opolskie. From Strzelce Opolskie we take road 409 to Kalinów and then turn south onto a local road to **Góra Sw. Anny** (**accomodation**). From Góra św. Anny we drive north by a local road and then west by road 409 to Gogolin (**Gogolin** quarry,

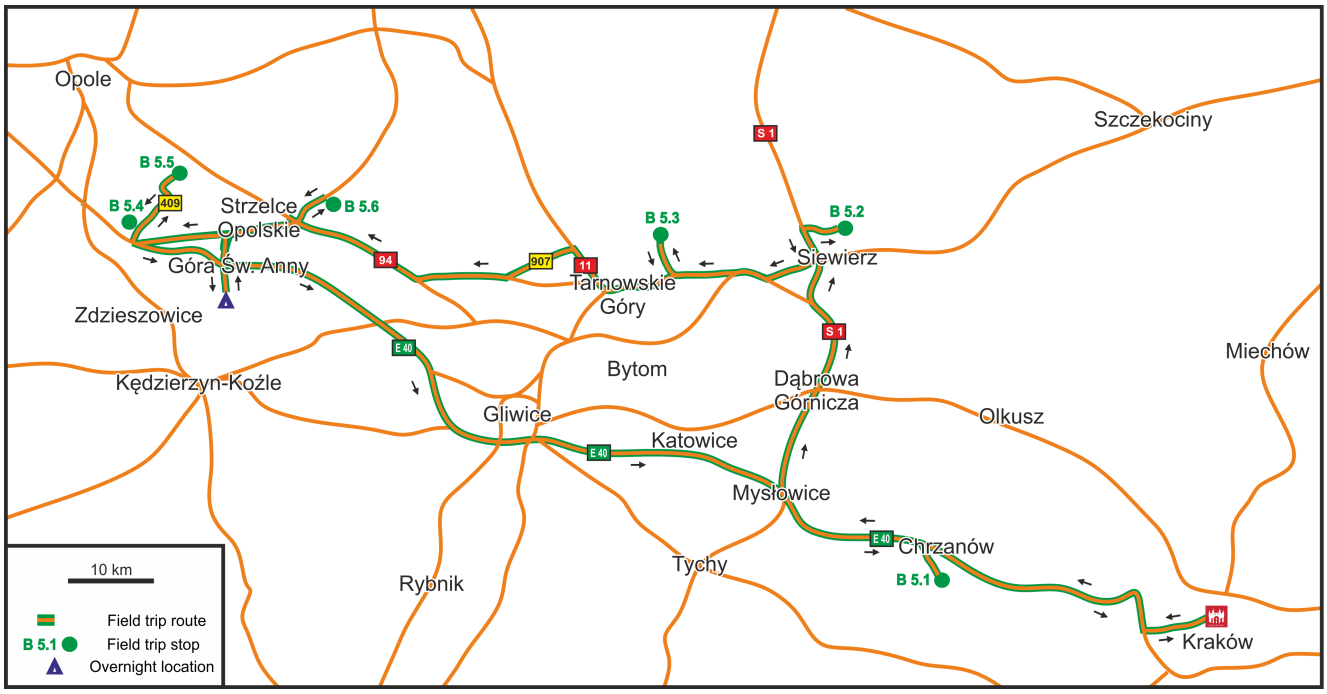

Fig. 1. Route map of field trip B5.

Szulc, J., Matysik, M. & Hagdorn, H., 2015. The Mid-Triassic Muschelkalk in southern Poland: shallow-marine carbonate sedimentation in a tectonically active basin. In: Haczewski, G. (ed.), *Guidebook for field trips accompanying IAS 31st Meeting of Sedimentology held in Kraków on 22nd–25th of June 2015*. Polish Geological Society, Kraków, pp. 195–216.
Guidebook is available online at www.ing.uj.edu.pl/ims2015

stop B5.4). From Gogolin we travel north by local roads to **Tarnów Opolski** (Opolwap-Lhoist quarry, **stop B5.5**) and then east by road 94 to **Strzelce Opolskie** (Heidelberg Cement quarry**, stop B5.6**). From Strzelce Opolskie we get to motorway A4 and return to Kraków.

Introduction to the trip

Tectonic setting of the eastern Peri-Tethys Basin in Triassic times

Joachim Szulc

During Triassic times Silesia was a SE part of the Germanic Basin which pertained to the northern periphery of the Western Tethys Ocean. The eastern part of the Germanic Basin was strongly influenced by reactivated Variscan structures which controlled the basin differentiation, subsidence pattern and Tethys-Peritethys palaeocirculation pattern in Triassic times (Fig. 2). The Silesian part of the Germanic Basin was controlled by the Silesian-Moravian Fault and the Kraków–Odra-Hamburg Fault (Fig. 2).

Synsedimentary tectonics, resulting in structural differentiation of the Germanic Basin, was active practically throughout the entire Triassic. In early Triassic several phases of block tectonics resulted in basinwide Buntsandstein discordances (Volpriehausen, Detfurth and Hardegsen unconformities). Migration of the Muschelkalk depocentre in Mid Triassic times from Central Poland to Central Germany is another example illustrating well the crustal mobility (Szulc, 2000). Differentiated crustal movements continued also in late Triassic producing several prominent tectonically induced unconformities (Beutler, 2005).

Apart from above mentioned, large-scale indicators of the basin tectonics, there are common direct evidences of syndepositional crustal mobility: small synsedimentary faults and dilatation cracks that developed within the Triassic deposits and reached the basement rocks, or seismically-induced liquefaction and fluidization phenomena visible already in Buntsandstein clastics (Schüler *et al.*, 1989). Seismically induced synsedimentary deformations are particularly common in the marine Muschelkalk

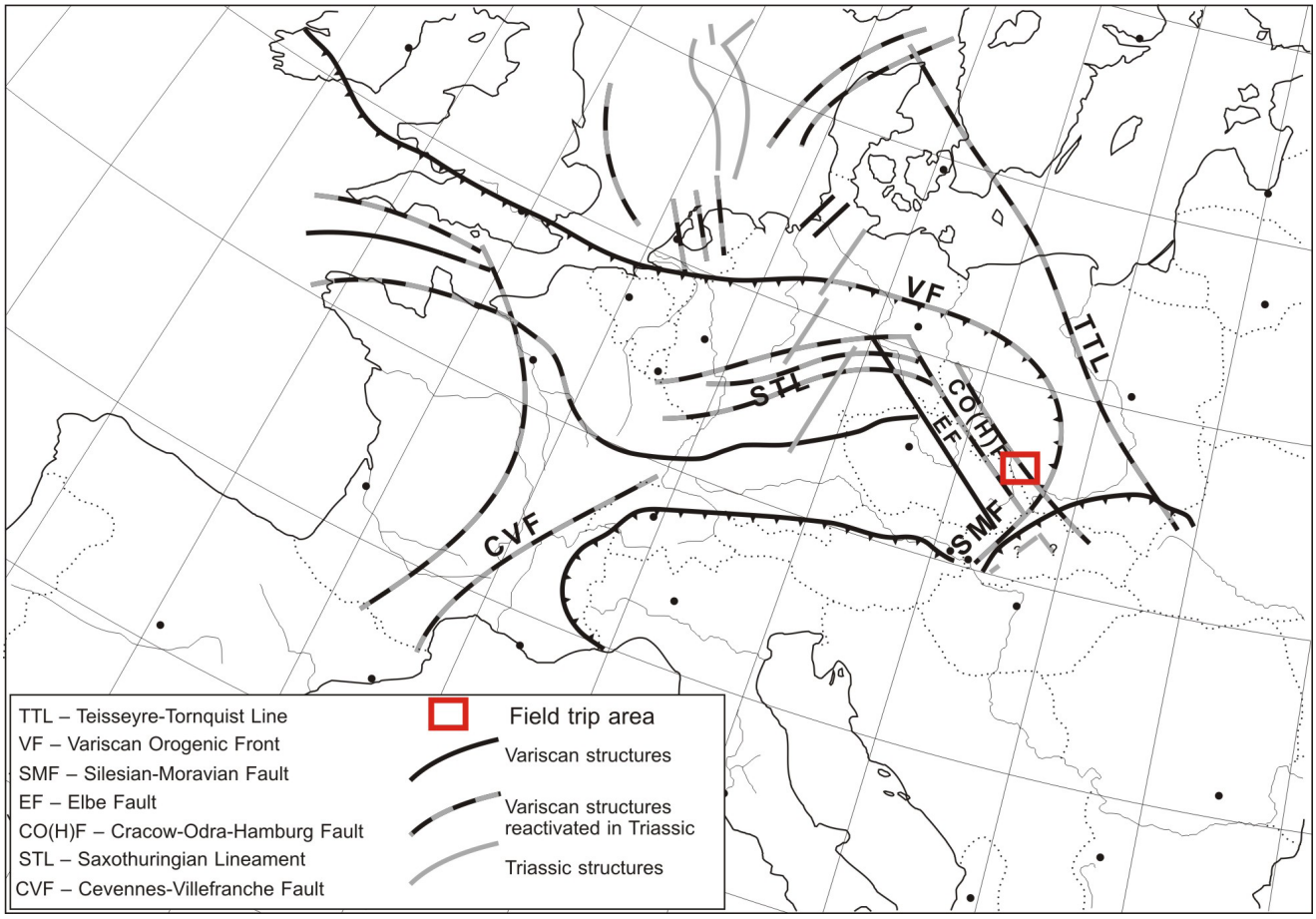

Fig. 2. Principal tectonic elements controlling the eastern part of the Germanic Basin in Triassic times.
TTL – Teiseyere-Tornquist Line, VF – Variscan orogenic front, SMF – Silesian-Moravian Fault; COH – Cracow-Hamburg Fault line; EF – Elbe Fault; STL – Saxothuringian Lineament. Trip area in red.

carbonates (Szulc, 1993; Voigt and Linnemann, 1996; Rüffer, 1996) and in Upper Triassic sediments (Szulc, 2005; Szulc *et al.*, 2006).

In spite of the intense tectonic activity the main eustatic pulses in the Triassic are generally well marked in the Peri-Tethys basins, in particular for the late Olenekian – early Carnian interval. Significant progress of sequence stratigraphy and magnetostratigraphy has improved the potential and reliability of dating and correlation of the most pronounced transgressive-regressive pulses recognized in the area. The sequence stratigraphic frameworks from the Alpine and Germanic basins display good correlation at the level of 3rd order sedimentary sequences (see discussion in Szulc, 2000). As became clear from very careful studies by Matysik (2014; 2015) the higher frequency cycles (4th and 5th order) are much more susceptible to local factors (storms, tectonics) hence an attempt of ascribing them to overregional controls (for instance to Milankovitch orbital rhythms) is a risky, speculative and unreliable procedure.

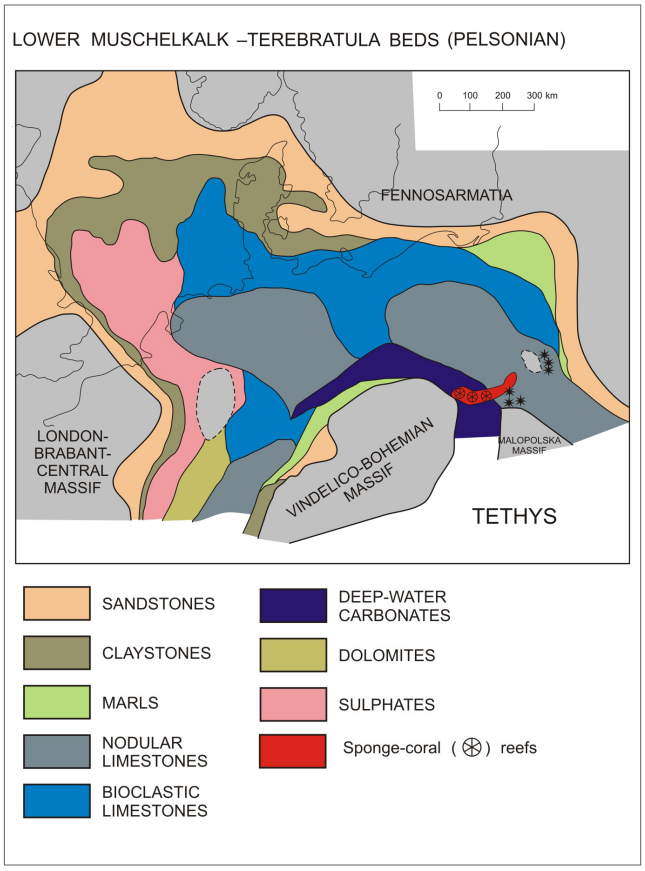

Fig. 3. Palaeofacies map of the Peri-Tethys domain for the Pelsonian interval (after Szulc, 2000).

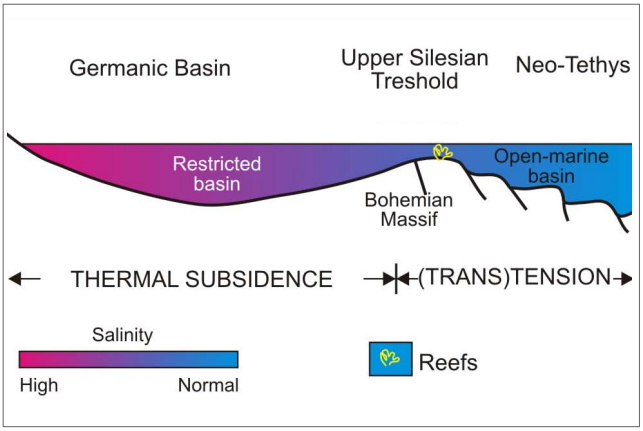

Fig. 4. Schematic model of basin dynamics and circulation regime in the Northern Peri-Tethys domain.

General setting of the Silesian Röt and Muschelkalk

Joachim Szulc

In late Olenekian time, a free communication between the Tethys and Germanic basins was established and the southernmost part of the Polish basin became an integral part of the Tethys Ocean. It concerns, first of all, the Upper Silesian area that formed tectonically mobile threshold block dividing the open ocean domain from a vast inner back-ramp "lagoonal" basin (i.e. Germanic Basin *s.s.*) (Fig. 4). Such configuration resulted in palaeocirculation pattern typical of semi-closed marine basins. Normal marine conditions dominated in the Upper Silesia, whereas northward and westward from the Silesian and East Carpathians domains the environments became more and more restricted. Marine incursions entered from the Tethys Ocean *via* the Silesian-Moravian Gate (SMG), while the other sides of the basin were closed. Normal marine water flowing from the SE accumulated in the depocentre and underwent evaporation, leading to halite/gypsum precipitation (Fig. 3).

Palaeoceanographic circulation pattern established in late Olenekian continued also in Anisian time. The main communication pathways between the Tethys and Germanic basins led through the SMG and East Carpathian Gate (ECG). Since Pelsonian time also the western, Allemanic Gate or (former Burgundy Gate), became active.

The basin reorganization commenced at the beginning of the Ladinian when intense crustal uplift in the eastern province resulted in an increase of clastic supply in uppermost Muschelkalk-Lower Keuper times and led finally to emersion and a stratigraphic hiatus encompassing the late Ladinian (Fassanian) interval.

Stratigraphy of the Silesian Röt-Muschelkalk and its correlation with the alpine Triassic

Joachim Szulc

Owing to free communication of the Silesian area with the open Tethys Ocean and common occurrence of the alpine index fossils (conodonts, ammonoids), the marine Röt – Muschelkalk succession in southern Poland acquires quite detailed biostratigraphy enabling its correlation with the Tethyan realm (Kozur, 1974; Trammer, 1975; Zawidzka, 1975; Brack *et al.*, 1999; Narkiewicz and Szulc, 2004).

Muschelkalk biostratigraphy has been improved by investigations on crinoids and echinoids, which appeared to be very useful tools for correlation with the Tethyan realm (Hagdorn and Głuchowski, 1993). Also palynofacies analysis has been used as a tool for basin-wide correlation and high-resolution sequence stratigraphic interpretation in the Middle Triassic of the Germanic realm (Götz *et al.*, 2005) as well as for correlation of depositional sequences of the northwestern Tethys shelf area with the northern Peri-Tethyan Basin (Götz *et al.*, 2005).

The Middle Muschelkak, devoid of conodonts and other index fossils, has been divided by Kotański (1994) into 6 dasycladacean zones. According to Kotański, the Pelsonian/Illyrian boundary lies in the lower part of the Diplopora Beds and is defined by first occurrence of several species of diplopores e.g., *D. annulatisima*, *D. silesiaca* and *D. multiserialis*.

The chronostratigraphical framework of the Röt – Muschelkalk (late Olenekian – early Ladinian) in southern Poland (Fig. 5) has been supported and refined by magnetostratigraphical and sequence stratigraphical studies (Nawrocki and Szulc, 2000; Szulc, 2000)

Evolution of the Silesian Basin in late Olenekian – early Ladinian times

Joachim Szulc

The Silesian basin experienced several transgression-regression events well illustrated by 3rd order depositional sequences setting (Fig. 5).

The Röt deposits encompass two 3rd order depositional sequences (Szulc, 2000). The first one is very well developed in Upper Silesia where it commences with

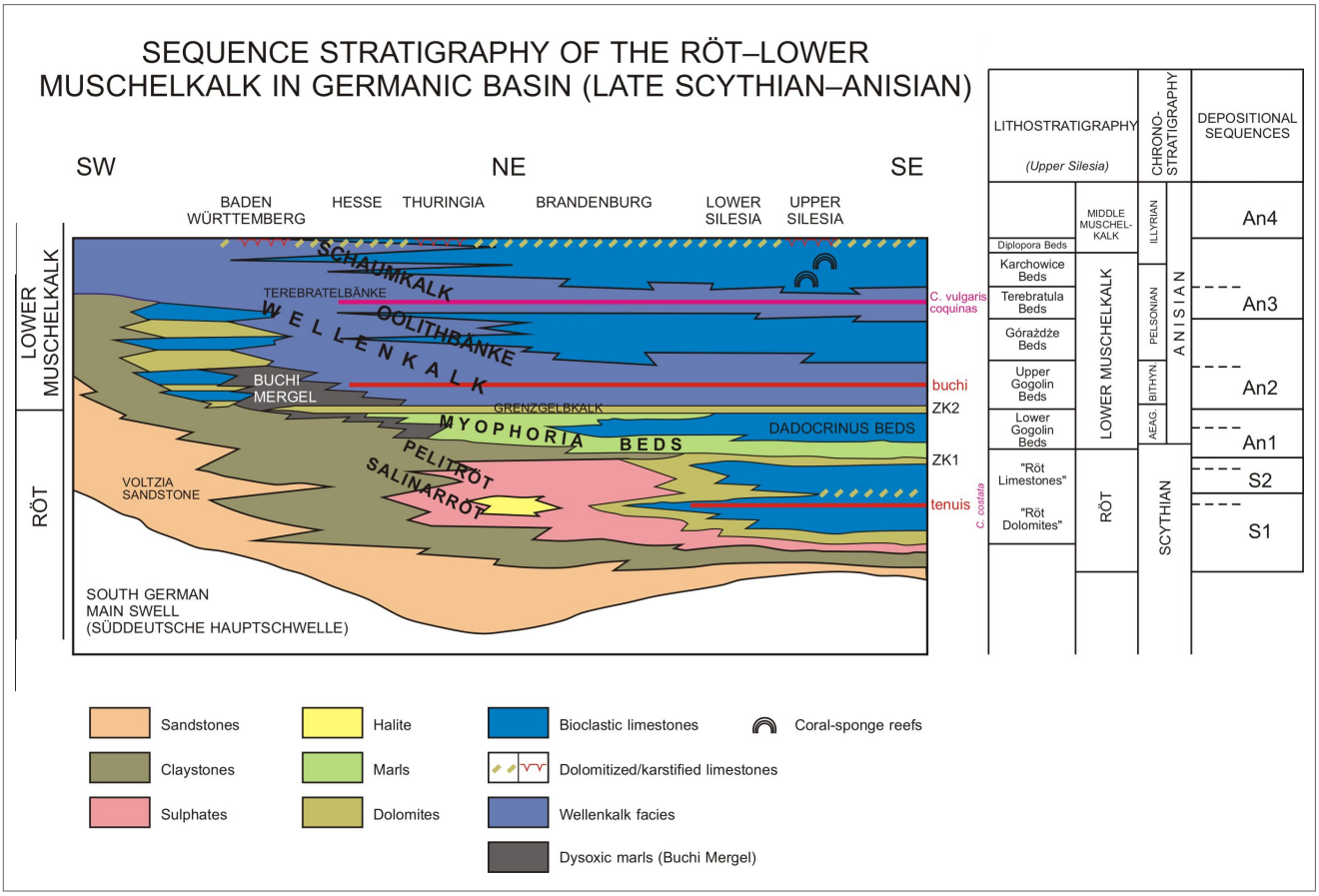

Fig. 5. Sequence-stratigraphic framework of the Lower Muschelkalk of the Germanic Basin (from Szulc, 2000).

fine-grained clastics followed by dolomites, sulphates and bioclastic and oolitic limestones. The carbonates contain relatively rich assemblages of gastropods and bivalves; *Costatoria costata* coquinas are dominant. Limestone beds in the upper part of the succession contain numerous cephalopods (*Beneckeia tenuis*) and crinoids that record the first maximum flooding stage (Fig. 5).

The second transgression in the Germanic Basin generally encompassed the same area as the first one. The lithofacies pattern shows a similar distribution; carbonate sedimentation was again dominant in the areas of the Silesian-Moravian and East Carpathian gates, while basinward both, dolomites and sulphates were deposited.

The Lower-Middle Muschelkalk is composed of four 3rd order depositional sequences.

Their boundaries are well defined by emersion horizons displaying features of meteoric diagenesis (dissolution, dolomitisation, karstification, palaeosoil and ferricrete formation).

The prograding global Anisian transgression is marked by some important events defining the maximum flooding zones of the subsequent depositional sequences i.e. An2 and An3. First appearance of index conodonts (e.g. *Neogondolella bulgarica, Neogondolella regale*, *Nicoraella kockeli*,) and Tethyan ammonoids (*Balatonites ottonis*, *Acrochordiceras*) is the most important bioevent defining the maximum flooding surface (MFS) of the An2 seuquence. These fossils date the of the An 2 sequence as coincidental with the beginning of the Pelsonian stage and have enabled a reliable correlation of the Muschelkalk deposits with the Tethyan successions.

The MFS of the 3rd Anisian sequence is characterized by explosive appearance of *Coenothyris vulgaris* brachiopods building the so-called Terebratula Beds (Fig. 5). According to sedimentological citeria (Szulc, 1993) and palynofacies data (Götz *et al*., 2005) the transgressive Terebratula Beds represent the Anisian maximum flooding surface recognized over the whole Germanic basin (Aigner and Bachmann, 1992; Szulc, 1995). Exceptionally great number of Tethyan faunal elements: brachiopods, pelecypods, echinoderms, conodonts, corals and dasycladales occurring in Silesia (Assmann, 1944; Hagdorn, 1991, Szulc, 2000) unequivocally indicates that during this interval, the communication between the Germanic Sea and Tethys Ocean reached its optimum.

In Upper Silesia the HST of the An3 sequence climaxed with sponge-coral-echinoderm buildups (Fig. 9). The Anisian (late Pelsonian-early Illyrian) buildups belong to the oldest *in situ* found, well dated scleractinans reefs. The hitherto gathered coral collection comprises specimens representing about 20 species (see Morycowa, 1988). The most frequent genera and bioherm constructors are: *Pamiroseris*, *Volzeia*, *Koilocoenia, Eckastraea* and solitary corals described as "*Montlivaltia*".

From the palaeobiogeographical point of view, the Silesian reef belt formed a Tethys marginal "reefal" rim dividing the offshore, Tethyan open marine zone from the backreef area (Fig. 4). Thus, it represents a fragment of the circum-Tethyan "reef" belt, that fortuitously avoided later subduction.

Final stages of the HST in Silesia are represented by *Girvanella* oncoliths, dasycladacean debrites and finally by oolitic bars which begin the basin-wide regression stage of the Middle Muschelkalk.

The Middle Muschelkalk in Silesia is represented by dolomites, sulphates and fossil-poor limestones diplaying common features of subaerial exposure.

The Upper Muschelkalk, poorly exposed in Silesia is built by dolomitic limestones followed by coquina deposits and condensed limestones.

The biostratigraphical data indicate that in the eastern parts of the Germanic basin, normal marine conditions have been replaced by brackish environments three conodont zones earlier than in southwestern Germany (Fassanian in Silesia *vs*. Longobardian in SW Germany) (Kozur, 1974; Trammer, 1975; Zawidzka, 1975; Narkiewicz and Szulc, 2004). The end of normal marine sedimentation in the Polish basin was coincidental with the *cycloides*-Bank *i.e.* with the maximum flooding phase of the Upper Muschelkalk in Germany.

Middle Triassic macrofauna in Silesia and its connection with the Tethys (Figs 6–9)

Hans Hagdorn

The Silesian Röt and Muschelkalk is widely known with its very rich fossil assemblage. It is noteworthy that the earliest descriptions of Triassic fossils from Upper Silesia, those by Meyer (1849), Dunker (1851) and Eck (1865), emphasized the close similarity of the Silesian

Muschelkalk with the alpine Triassic. In reviews of the Upper Silesian Muschelkalk faunas, Ahlburg (1906) and Assmann (1913, 1915, 1924, 1925, 1927, 1937, 1944) demonstrated that the percentage of Tethyan macrofaunal elements reached its peak in the Karchowice Beds and in the Diplopora Dolomite i.e. in the formations representing the maximum transgression stage in Anisian (Pelsonian). These data were supported also by later microfauna studies of condonts (Kozur, 1974; Zawidzka, 1975; Narkiewicz and Szulc, 2004).

The earliest marine ingression in Triassic times reached southeastern Poland during the late Olenekian when the Röt Dolomite was deposited. Its fauna is dominated by the myophoriid bivalve *Costatoria costata* and by the modiolids (*Modiolus* (?) *triquetrus).* Additional common fossils are the bakevelliids (*Hoernesia socialis* and *Bakevellia costata)*, the pectinoid *Leptochondria albertii*, *Pseudomyoconcha gastrochana*, the gastropod *Wortheniella* and the hedenstroemiid ammonoid *Beneckeia tenuis).* It is worth to note that some crinoid remains have been found in the Röt of southern Silesia (Alexandrowicz and Siedlecki, 1960). By means of *Costatoria costata*, the Röt Dolomite has already been correlated by Eck (1865) with the Werfen Formation of the Tethyan Triassic, though *Beneckeia* has not been found there.

Due to normal salinity and a greater variety of substrates, the Muschelkalk faunas are much more diverse than the Röt ones. The diversity depends on the progressive opening of the marine gates that connected the Central European Basin with the Tethys. Generally, in late Anisian (Pelsonian and early Illyrian) times, Silesia rather belonged to the Tethyan faunal domain than to the epicontinental Germanic province.

The lowermost Muschelkalk (Gogolin Beds), displays massive occurrence of stenohaline crinoids (*Dadocrinus* sp., *Holocrinus acutangulus,* evidencing normal marine environments. The crinoids were accompanied by ophiuroids (*Aspiduriella*, *Arenorbis*), mudsticking bivalves like *Bakevellia mytiloides*, *Hoernesia socialis*, *Pseudomyoconcha*, the myophoriids *Myophoria vulgaris*, *Neoschizodus laevigatus*, *Elegantinia elegans*, *Pseudocorbula*, *Pleuromya cf. fassaensis*, the gastropod *Omphaloptycha gregaria* and the nautiloids *Germanonautilus dolomiticus* and *G. salinarius* and, more rarely, the ammonoids, *Beneckeia buchi*, *Noetlingites strombecki*, *Balatonites ottonis*, *Acrochordiceras* that allow correlation with the Anisian Angolo Limestone of the Southern Alps.

During the Pelsonian communication between the Tethys and Silesia reached its climax as suggests common occurrence of the typical Tethyan cephalopods *Pleuronautilus planki*, *Balatonites*, *Bulogites* and *Paraceratites*, articulate brachiopods *Tetractinella trigonella*, *Mentzelia mentzeli*, and *Decurtella decurtata* as well as the dasycladacean green alga *Gyroporella minutula*. This is especially true for the corals (more than 20 species, including *Volzeia szulci* (Fig. 9c), *Pamiroseris silesiaca* (Fig. 9b), *Eckastraea prisca,* "*Montlivaltia*") and hexactinellid sponges (*Tremadictyon*, *Calycomorpha*, and *Silesiaspongia* and *Hexactinoderma*) that built the first, dated Mesozoic reefs after the P/T reefbuilders extinction.

The wealth of echinoderms also clearly indicates the Tethyan realm. Additionally to the encrinids *Encrinus robustus*, *E.* cf. *aculeatus*, *Carnallicrinus carnalli*, *Chelocrinus* sp. indet., and *Holocrinus dubius* that were dispersed over the entire Muschelkalk Basin, typical *Encrinus aculeatus*, *E. spinosus*, *Holocrinus meyeri*, *Eckicrinus radiates*, and the poorly known *Silesiacrinus silesiacus* are Tethyan crinoids that are also found in the Alps (Recoaro Fm.) and in Hungary (Hagdorn and Gluchowski 1993).

According to Assmann (1944), the bivalve fauna comprises 44 species, among which 15 are endemic in Upper Silesia, 12 are exclusively Germanic Muschelkalk, 4 are Alpine, and 13 occur in both the Alpine and the Germanic provinces. Among the 33 gastropod species, the Tethyan influence is even more evident. However, two thirds of the gastropod taxa, many of which have been found in a single specimen only, are endemic to Upper Silesia, 5 species are Alpine and 2 are Germanic. The most remarkable elements are large, ornamented archaeogastropods that inhabited the reefs.

In contrast to the Lower Muschelkalk the Middle and Upper Muschelkalk of Silesia is much poorer in number and species of invertebrate fossils and is dominated by germanotype faunal elements.

Syndepositional record of seismic activity in the Muschelkalk basin

Joachim Szulc

Earthquake events are commonly recognized as a trigger mechanism of mass movements in both, conti-

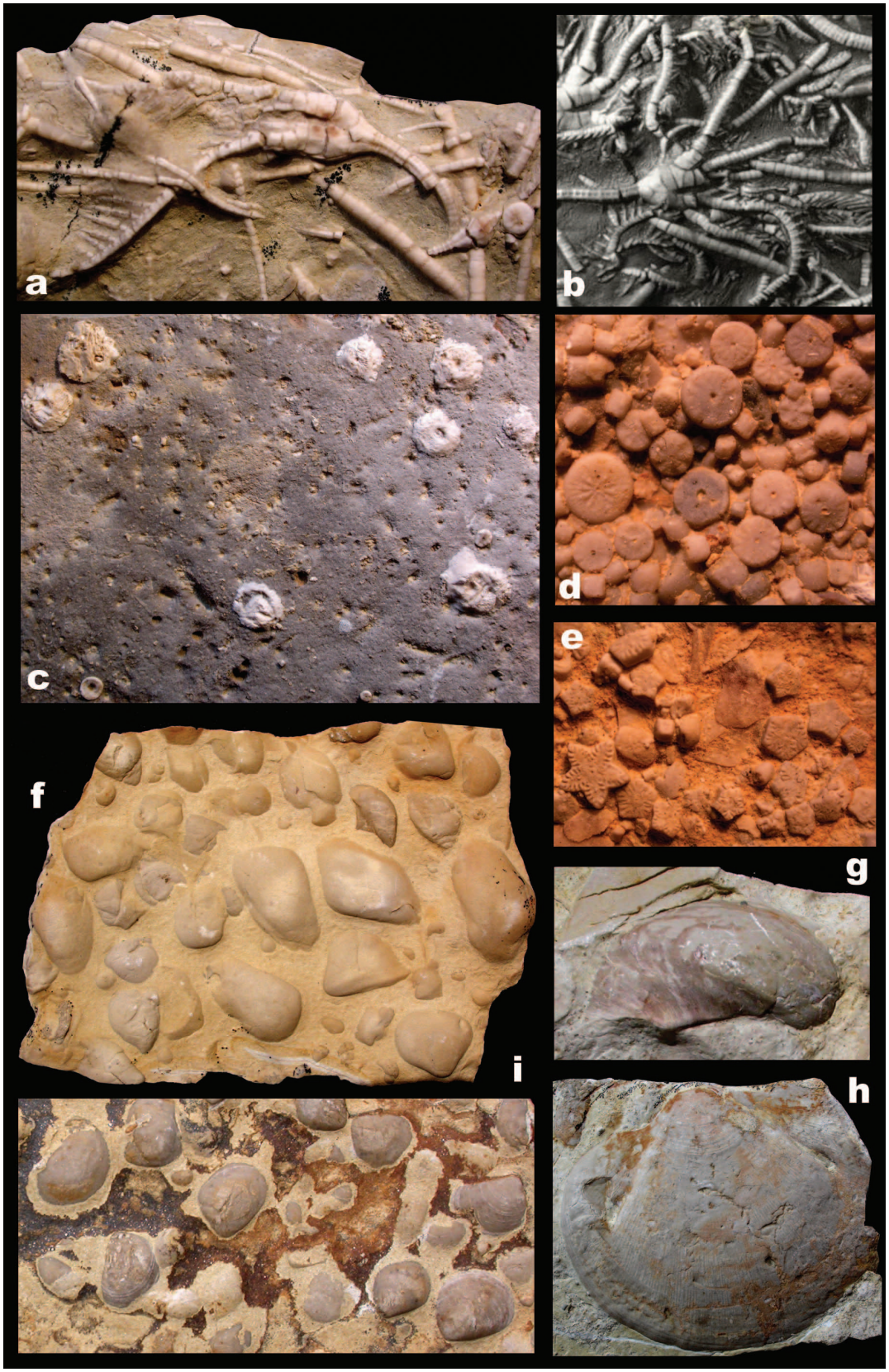

Fig. 6. Fauna of the Gogolin Formation. **a.** *Dadocrinus* sp., crown and stem fragments of a small, still undescribed dadocrinid from the Lower Gogolin Fm. of Milowice (x 2,5). **b.** *Dadocrinus kunischi*, the largest dadocrinid. Lower Gogolin Fm., Gogolin (x 0,8). **c.** Holdfasts of dadocrinids on top of a large intraclast; note the openings of *Trypanites* borings. Lower Gogolin Fm., Ząbkowice Bedzinskie (x 1). **d.** Dadocrinid columnals, Lower Gogolin Fm., Zyglin (x 2,5). **e.** *Holocrinus acutangulus*, columnals. Upper Gogolin Fm., Wojkowice Komorne (x 2,5). **f.** Soft bottom palaeocommunity of *Arcomya* cf. *fassaensis*, *Myophoria vulgaris*, *Bakevellia costata*, *Omphaloptycha gregaria*. Lower Gogolin Fm., Żyglin (x 0,8). **g.** *Hoernesia socialis*. Lower Gogolin Fm., Gogolin (x 1). **h.** *Entolium* cf. *E. discites*. Lower Gogolin Fm., Wojkowice Komorne (x 0,6). **i.** *Plagiostoma beyrichi*. Upper Gogolin Fm., Plaza (x 1). All specimens Muschelkalkmuseum Ingelfingen.

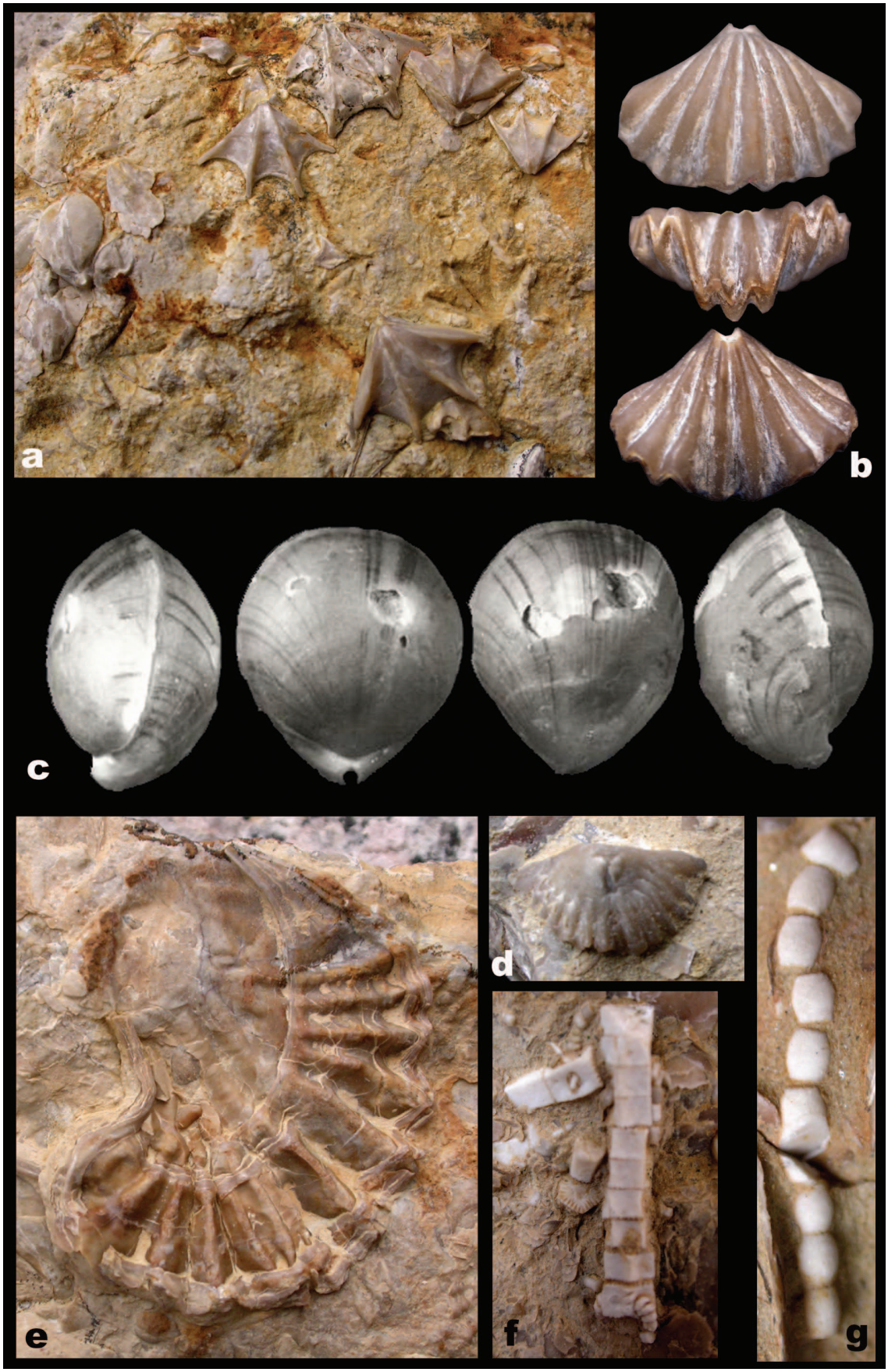

Fig. 7. Fauna of Terebratula Beds (Dziewkowice Formation). **a.** *Tetractinella trigonella, Silesiathyris angusta.* Strzelce Opolskie (x 2). **b.** .*Decurtella decurtata.* Strzelce Opolskie (x 3,8). **c.** *Coenothyris vulgaris*, with color bands. Strzelce Opolskie (x 1,7). **d.** *Hirsutella hirsuta.* Gorazdze (x 3). **e.** *Umbrostrea difformis.* Strzelce Opolskie (x 2). **f.** *Holocrinus dubius*, noditaxis of 10 columnals, with a cirrinodal at its lower end indicating an intermediate stage of disarticulation. Strzelce Opolskie (x 3,4). **g.** Indeterminate encrinid or dadocrinid with barrel-shaped columnals. Strzelce Opolskie (x 5). All specimens Muschelkalkmuseum Ingelfingen.

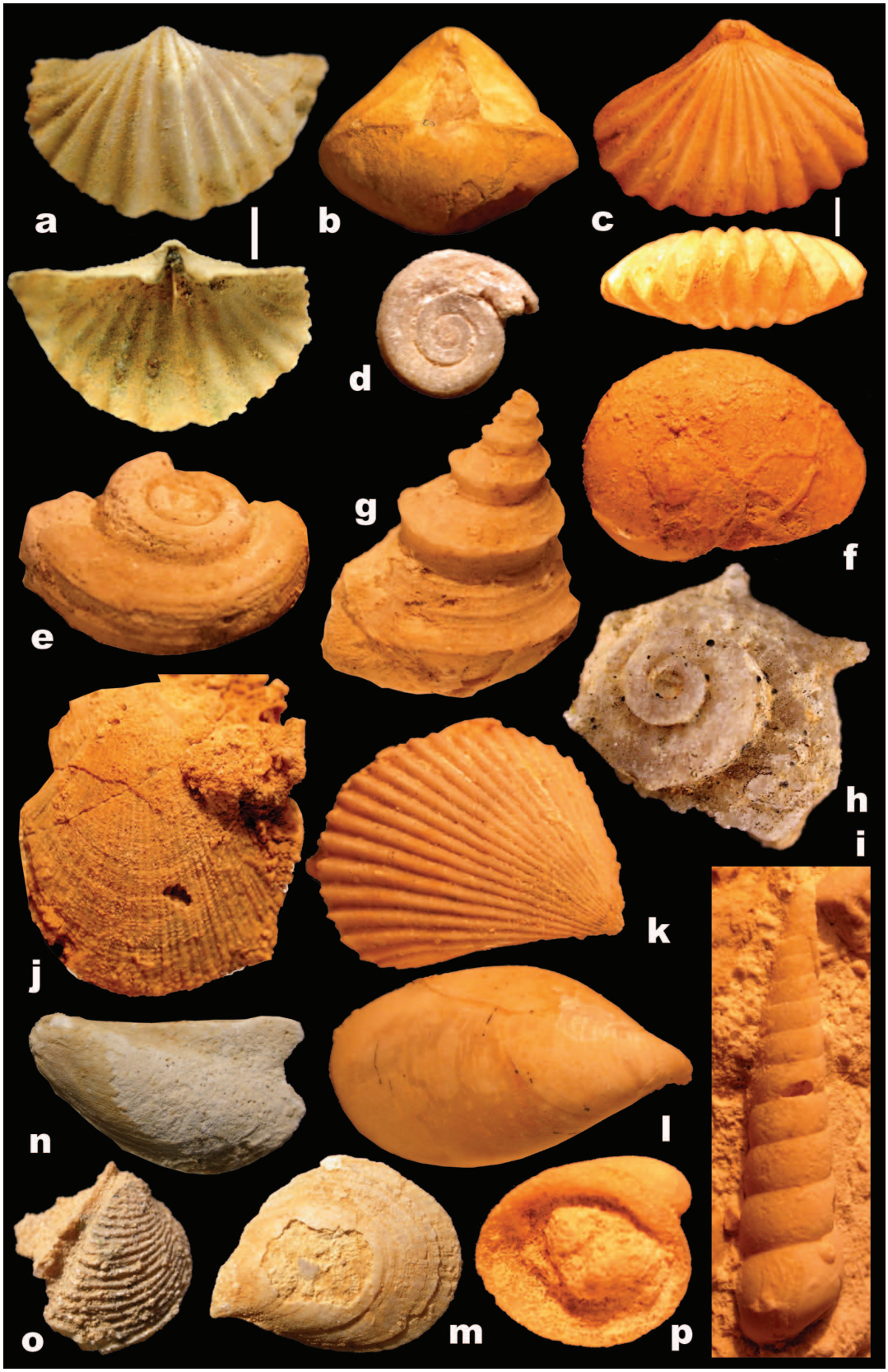

Fig. 8. Brachiopods, gastropods, and bivalves of the Karchowice Formation. **a.** *Punctospirella fragilis*, pedicle valve. Strzelce Opolskie (x 2,5). **b.** *Mentzelia mentzeli*. Tarnów Opolski (x 3,5). **c.** *Costirhynchopsis mentzeli*. Tarnów Opolski (x 3). **d.** *Discohelix (Amphitomaria) arietina*. Tarnów Opolski. (x 6) **e.** *Euomphalus semiplanus*. Tarnów Opolski (x 3,3). **f.** *Neritaria* cf. *N. comensis*, with encrusting serpulid (?). Tarnów Opolski (x 2,5). **g.** *Wortheniella* sp. Tarnów Opolski (x 2). **h.** *Coelocentrus silesiacus*. Tarnów Opolski (x 3,8). **i.** *Trypanostylus* sp. Tarnów Opolski (x 4). **j.** *Praechlamys schroeteri*. Strzelce Opolskie (x 2,5). **k.** *Lima acutecostata*. Strzelce Opolskie (x 2,5). **l.** *Promysidiella praecursor*. Tarnów Opolski (x 2). **m.** *Mysidioptera fassaensis*. Tarnów Opolski (x 2,5). **n.** *Bakevellia* cf. *B. costata*. Tarnów Opolski (x 2). **o.** *Elegantinia elegans*. Tarnów Opolski (x 2,5). **p.** *Schafhaeutlia* sp. Tarnów Opolski (x 5). All specimens Muschelkalkmuseum Ingelfingen.

Fig. 9. Sponges and corals of the Karchowice Formation.
a. *Silesiaspongia rimosa*. Strzelce Opolskie (x 2,2). **b.** *Pamiroseris silesiaca*. Tarnów Opolski (x 2,5). **c.** *Volzeia szulci*. Tarnów Opolski (x 2,8). **d.** *Coelocoenia exporrecta*. Strzelce Opolskie. (x 2). **e.** *Pinacophyllum* (?). Tarnów Opolski (x 2). **f.** *Montlivaltia* (?). Tarnów Opolski (x 2,5). All specimens Muschelkalkmuseum Ingelfingen.

nental and submarine environments. However, the resulted gravity mass-transported deposits: rockfalls, debris flows, slumps and turbidites are sedimentary fabrics that may originate also without seismic stimulus, but may be caused by other factors e.g. slope failure by overload or by impact of storm waves. In order to avoid misinterpretation of sedimentary structures postulated as seismically-induced fabrics, they should be always referred to their sedimentary context. Such circumstantial criteria as geodynamic position of the basin (tectonically active *vs.* passive), very abrupt lateral and vertical facies succession, basin geometry (gentle slopes) and first of all, some indicative deformational structures are arguments in favour of unequivocal palaeoseismic interpretations.

The Muschelkalk basin was situated in the northern periphery of the rifted Tethys Ocean and gentle sloped ramp geometries dominated over the basin. Sedimentary sequences of the Muschelkalk are mostly composed of fine-grained carbonates (*Wellenkalk* facies) with subordinate contribution of coarse bioclastic and biolithic limestones and evaporites. As discussed above, the basin was influenced by syndepositional tectonism related to activity of several master faults that transmitted the crustal motion produced in the Tethys intra-rift belt into its peripheries (Szulc, 1993, 2000).

Synsedimentary seismic activity in the Muschelkalk basin has long been postulated on the grounds of common plastic deformations of limestones (Schwarz, 1970). Comprehensive list of structures unequivocally evidencing seismic controls of the Muschelkalk basin has first been presented by Szulc (1993).

The most undoubted evidence of syndepositionary seismicity are phenomenona of sediment liquefaction and fluidization. In contrats to loosely packed siliciclastic deposits, early cementation of carbonates promotes their plasticity, hence the affected young lime sediments (fine-grained carbonates in particular) behave in a soft or ductile way. This in turn, favours development of plastic, cohesive deformations such as creeping, glides or slumping of material that has not undergone liquefaction and did not lose completely its original sedimentary attributes such as bedding or lamination. The ductile reaction makes the carbonates a natural sensitive seismograph, capable of precise recording of seismic tremors.

Faults, joints, breccias, neptunian and injection dykes

The synsedimentary faults in the Muschelkalk carbonates range in scale from a few centimeters to several meters (Figs 10A, 11A–C). Small scale brittle defomations are represented by slicken-sided faulting and sigmoidal fracturing (Fig. 10D–F). The brittle faults affected completely lithified carbonates but they are commonly accompanied by contemporaneous breccias and by flowage of the unconsolidated sediments (Fig. 11G–I). A particularly interesting example comes from eastern Silesia where an archipelago of fault-bounded islands linking a transpression zone developed in Middle Triassic times (Szulc, 1991). The uplifted Paleozoic basement rocks over there, display cracking veinlets (Fig. 10C–D) originated by hydraulic fracturing typical of earthquake relaxation (Masson, 1972).

Non-displacive deformations

This type of deformation is conspicuous by lack of any vertical and lateral translation of the deformed sediments. These deformations occur either as isolated crumples or as nodular, crumpled clusters and they range from several centimeters to 1 meter in size. (Fig. 12A–C). The crumpled fabrics adjoin directly the undeformed, stratified sediments. On the other hand, the deformations match generally the joint pattern of the encompassing rocks. This may be interpreted as an effect of incongruent progress of carbonate cementation. The unlithified carbonates became deformed plastically and/or homogenized in isolated centers while the completely lithified sediment underwent brittle jointing (Fig. 12A–B).

Load deformations

At first glance, the load structures look similar to the non-displacive deformations. However unlike the latter, the load deformations display obvious vertical translation, depending essentially on sinking of coarser-grained deposits (mostly calcarenites and calcisiltites) into lime muds (Fig. 12D–F).

Fault-graded beds

Seilacher (1969) was the first who ascribed this complex deformation to seismic trigger and named it. The deformations reflect consolidation gradient in quake-affected sedi-

ments. As a rule, the older, consolidated part undergoes brittle fracturing while the younger, semiconsolidated and/or unconsolidated tiers respond by ductile flowage or complete homogenization. The fault-graded beds are well developed in fine-grained, thin-stratified limestones of the Silesian Muschelkalk (Fig. 11G–H). Like the stationary deformations, this type of deformations is a very convincing diagnostic feature of palaeo-earthquake shocks. The presented tiering of disintegration is characteristic for lime sediments displaying progressive lithification.

Quake- induced sedimentary structures

For the following considerations, it is worth of notion that the basin floor had very gentle (<0.5°) or even flat floor with low hummocks (up to 2-3 m high) produced by storm waves and currents or built by colonial organisms (e.g. brachiopods or oysters). Such geometry predestinated slow, cohesive mass displacements rather than incoherent, gravity grain-flow transport. Indeed, in the Muschelkalk sedimentary sequences the elastic and plastic translations predominated, whilst the cohesionless redeposition was less frequent and is represented exclusively by high-density debris flow deposits.

The mass movements were initiated mostly by synsedimentary faulting which involved deplacement of nearby sediments. The faults exhibit both normal (mostly listric) and reversed sense of dislocation (Fig. 14). Depending on the consolidation stage and mechanical properties (competent *vs.* incompetent) of the affected sediments, various deformations originated along the drag plane. The unconsolidated deposits behave plastically (creeping) while the semiconsolidated (competent) limestones responded by gliding (Fig. 11J–L).

The slumps show rotational sliding of thick (up to 4m) packages of ductile lime mud. During sliding the mud underwent multiple overfolding giving very complex internal features of the slumping horizons (Fig. 11M) which could be correlated over the distance of several tens of km. Depth range of the faults rarely exceeds 2 m and they fade shortly.

The debris flows have been observed in the intervals of notably intense tectonic activity in the basin, which correspond to the beginning and the maximum stages of the Lower Muschelkalk transgression. Both sequences consist of intercalated limestone and marl beds. During a quake the lithified limestones ruptured, while unconsolidated marls underwent liquefaction and served as an easy-slip medium. If the distance of redeposition was relatively short, the failed horizon became a completely jumbled mass of broken fragments carried in more movable material (Fig. 13A–G). By a longer translation, the debris was fractionated by flotation of the lighter components and the basal angular slabs were shingled downslope (Fig. 13C). The largest slabs may reach 5 m in size. Lower boundaries of the debris-flows are sharp and rugged since the subjacent beds were distorted by drag and bulldozing as the moving mass was emplaced.

Tsunami deposits and the S-T dyads

Fossil tsunami deposits as gravity flow deposits are difficult to recognize without their reference to the sedimentary context and the associated deformational structures. In general, the most conceivable tsunamites are the graded beds following directly quake-induced deformations (Fig. 13). In the Silesian Muschelkalk basin such coupled occurrence of earthquake-induced deformations and associated tsunami deposits has first been recognized in the Silesian basin and called *Seismite-Tsunamite Dyad* or *S-T dyad* (Szulc, 1993; Fig. 13E–G). Composition of the S-T dyads changes upsection and reflects the transgressive trend in the basin. In the lower part, corresponding to the initial phase of transgression, the quake-induced slumps and debris-flow packages are covered with current transported, onshore and land-derived material. The last-named consists of rewashed red kaolinite clays evidencing its continental provenance (Figs 13E–F). In the basinal facies representing the maximum flooding event, the slumped, fossils-poor lime muds, are eroded and covered by graded, bioclastic debris (Fig. 13G).

Bipartite coquina beds are another example of seismically induced sedimentary structures (Fig. 13H). The beds represent a coupled sequence consisting of lower horizon of convex-down authochthonous shells entombed in lime mud (seismite) and the superjacent part composed of current-transported allochthonous skeletal debris, with shells settled in convex-up position (tsunamite).

Stop descriptions

Please note that almost all stops (beside stop B 5.4.) are situated in active quarries where permission for access is required

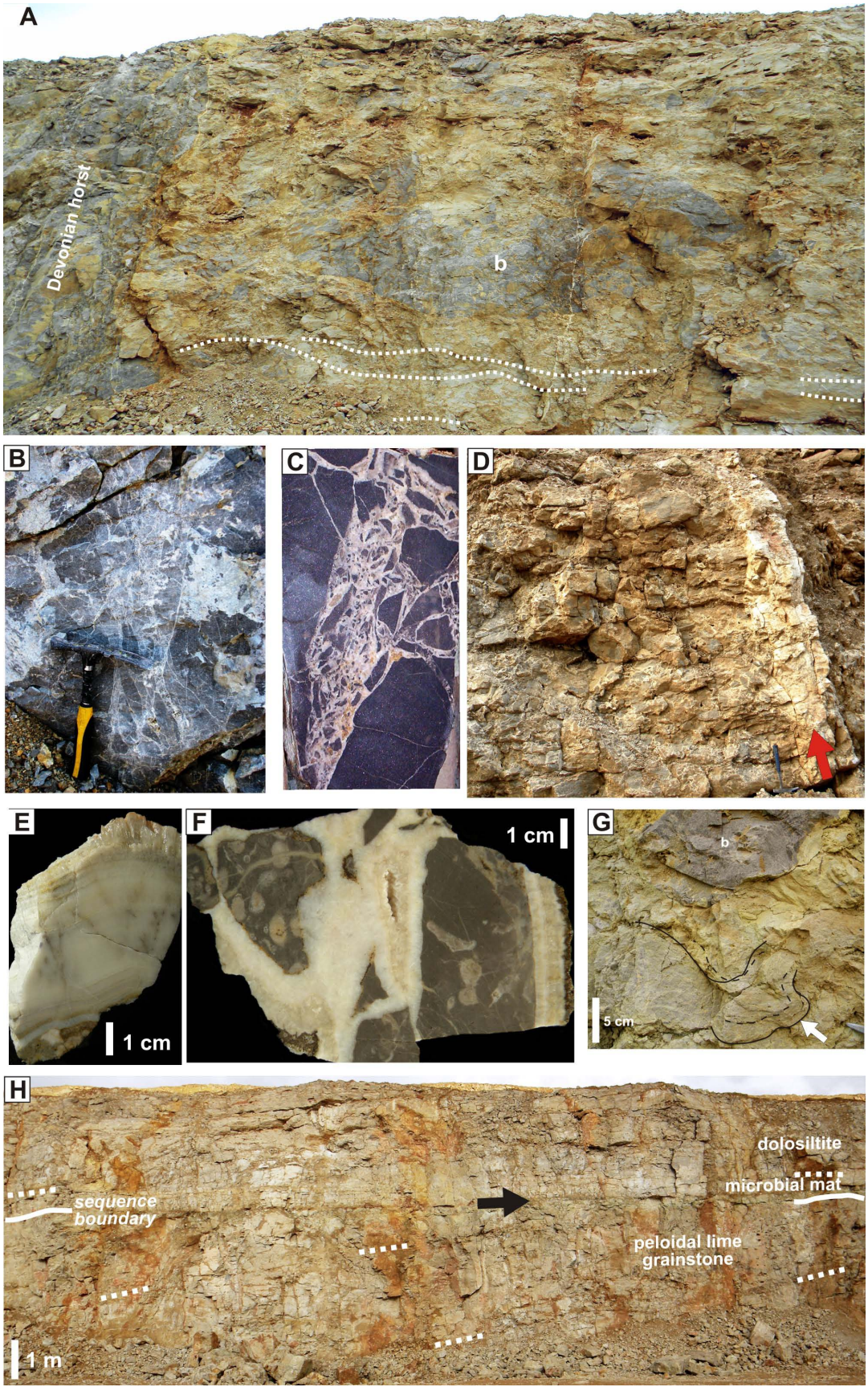

Fig. 10. Manifestation of synsedimentary tectonics in the GZD quarry, Nowa Wioska. Fault scarp and 7-m block of Devonian rocks (b) fallen to unlithified Triassic sediments. Note plastic deformation of the substrate. **A** – Hydraulic breccia developed in lagoonal dolomites, **B** – Details from Fig. 10 A, **C** – Outcrop view of a 40 cm-thick calcite vein (red arrow) piercing the Givetian black dolomites, **D** – Close up of the vein, **E** – Dissolution vugs filled with hydrothermal dolomite fill, **F** – 50 cm-large boulder of Devonian dolostone (b) deforming the underlying laminated Triassic calcarenites, **G** – Angular disconformity between 2nd and 3rd Anisian sequences (Olkusz Beds/Diplopora Beds).

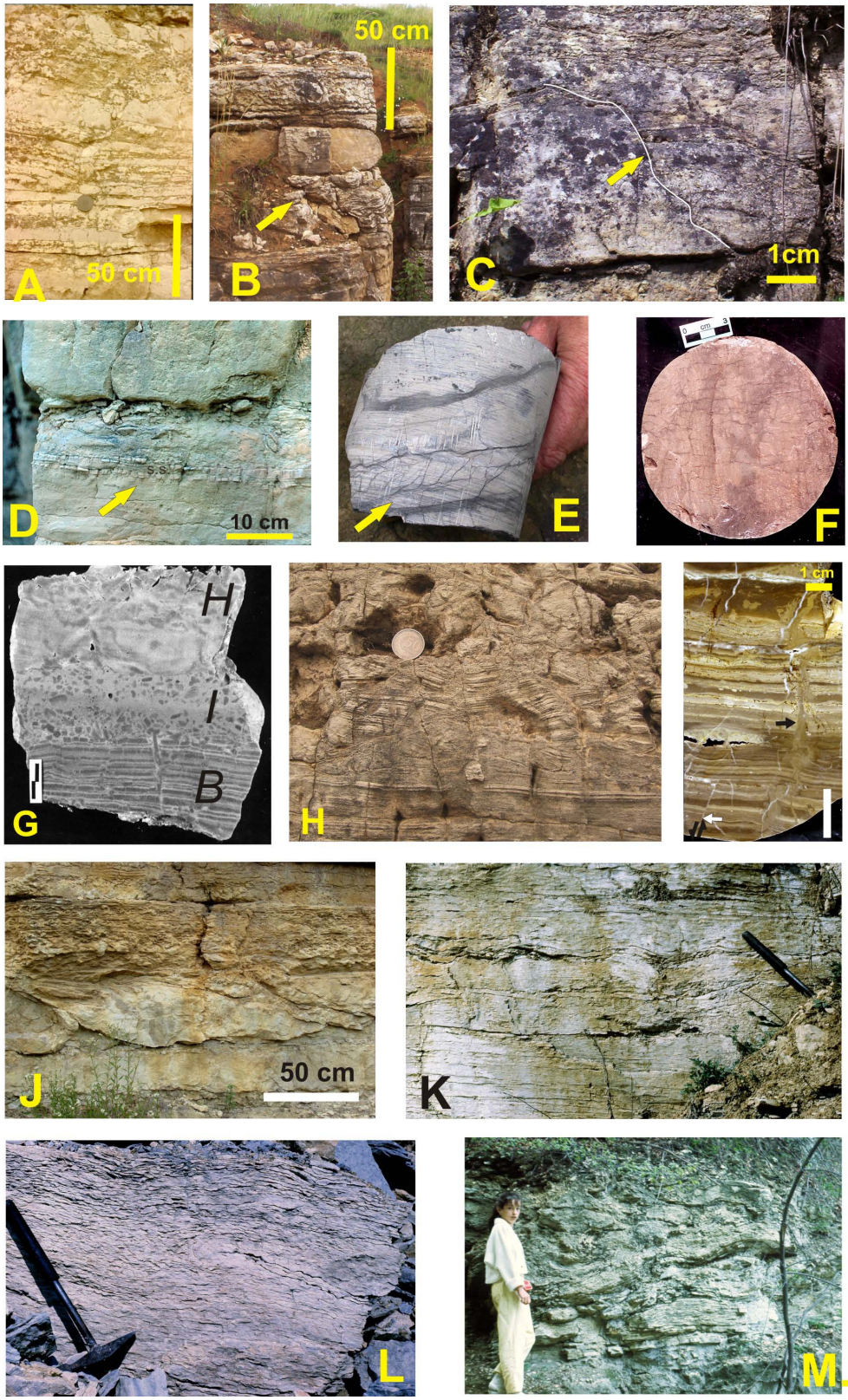

Fig. 11. Brittle and plastic quake-related deformations affecting the Muschelkalk limestones. **A** – Synsedimentary fault in Lower Gogolin Beds. Gogolin quarry, **B** – Synsedimentary fault in Gorażdże Beds, Naplatki quarry, **C** – Synsedimentary fault (arrow) in Lower Gogolin Beds, Libiąż, **D** – Slicken-sided faults (arrow) from Diplopora Beds. Libiąż quarry, **E** – Sigmoidal joints in Lower Muschelkalk. Gorzów Wielkopolski borehole, **F** – Plane view of joints from Fig. 11E, **G** – Fault-graded bed. Gogolin Beds, Płaza quarry. *B*- brittle fracturing, *H*- homogenisation, *I* – intermediate deformations, **H** – Quake-realted small synsedimentary faults, Górażdże Beds, Szymiszów quarry, **I** – Liquefaction injection dyke cutting microbial mats (black arrow). GZD quarry, Nowa Wioska, **J** – Synsedimentary intraformational slide slabs within the Górażdże Beds, Dąbrówka quarry, **K** – Gliding deformations from Terebratula Beds. Strzelce Opolskie quarry, **L** – Gliding and creeping deformations from Terebratula Beds. Strzelce Opolskie quarry, **M** – Overfolded and distorted limestones, Terebratula Beds. Góra św. Anny.

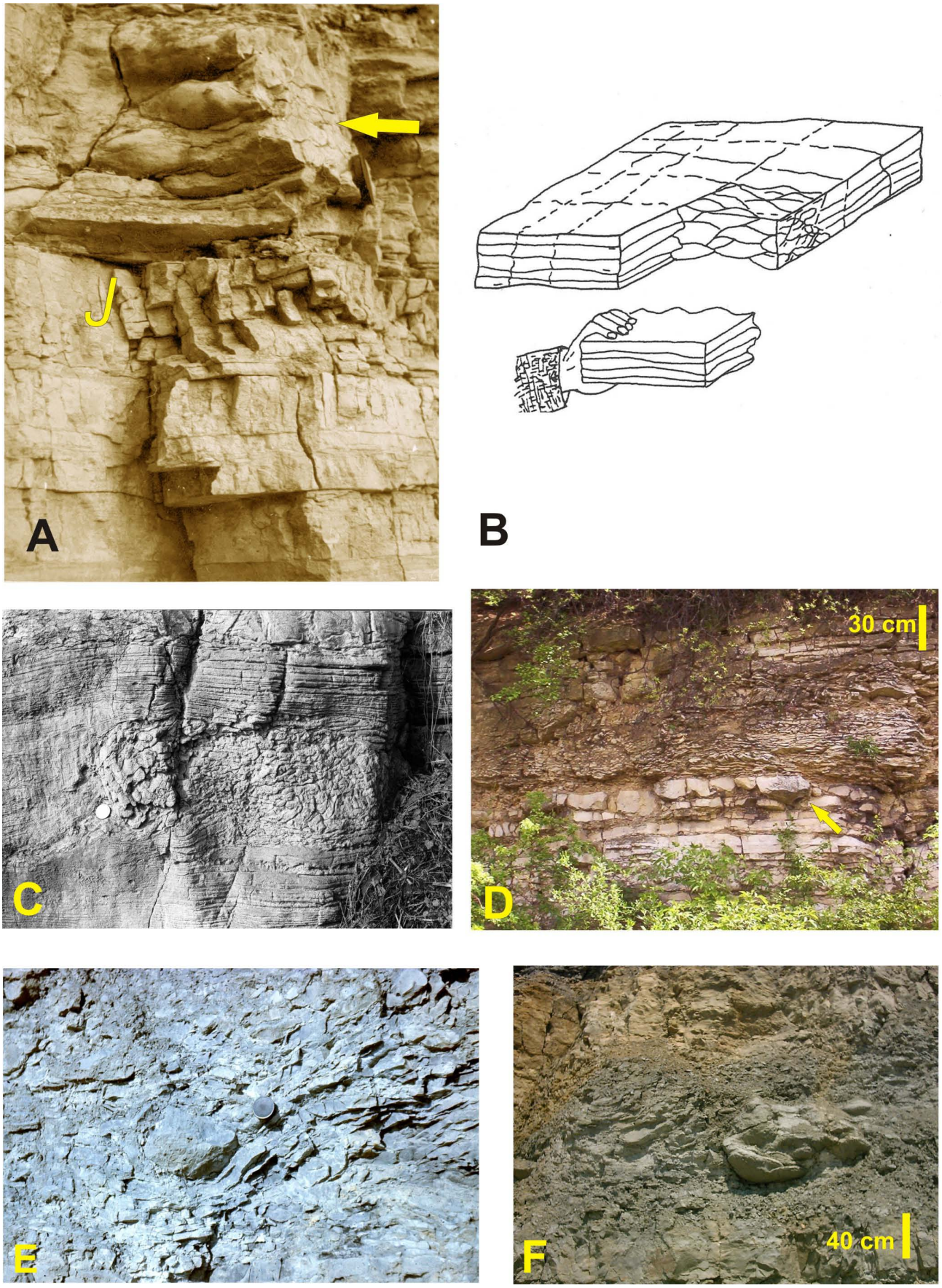

Fig. 12. Sedimentary and deformations related to Triassic synsedimentary tectonic activity in southern Poland. **A-B**. Photograph and drawing of non-displacive crumpled seismic deformations and joints, Lower Gogolin Beds. Gogolin, **C** – In-place crumpled seismic deformations. Gorażdże Beds, Raciborowice quarry, Lower Silesia, **D** – Load deformations from Gogolin Beds in Libiąż quarry, **E** – Isolated ball of calcarenites entombed in soft lime muds. Strzelce Opolskie quarry, **F** – Brachiopods colony sunken in lime muds. Strzelce Opolskie quarry.

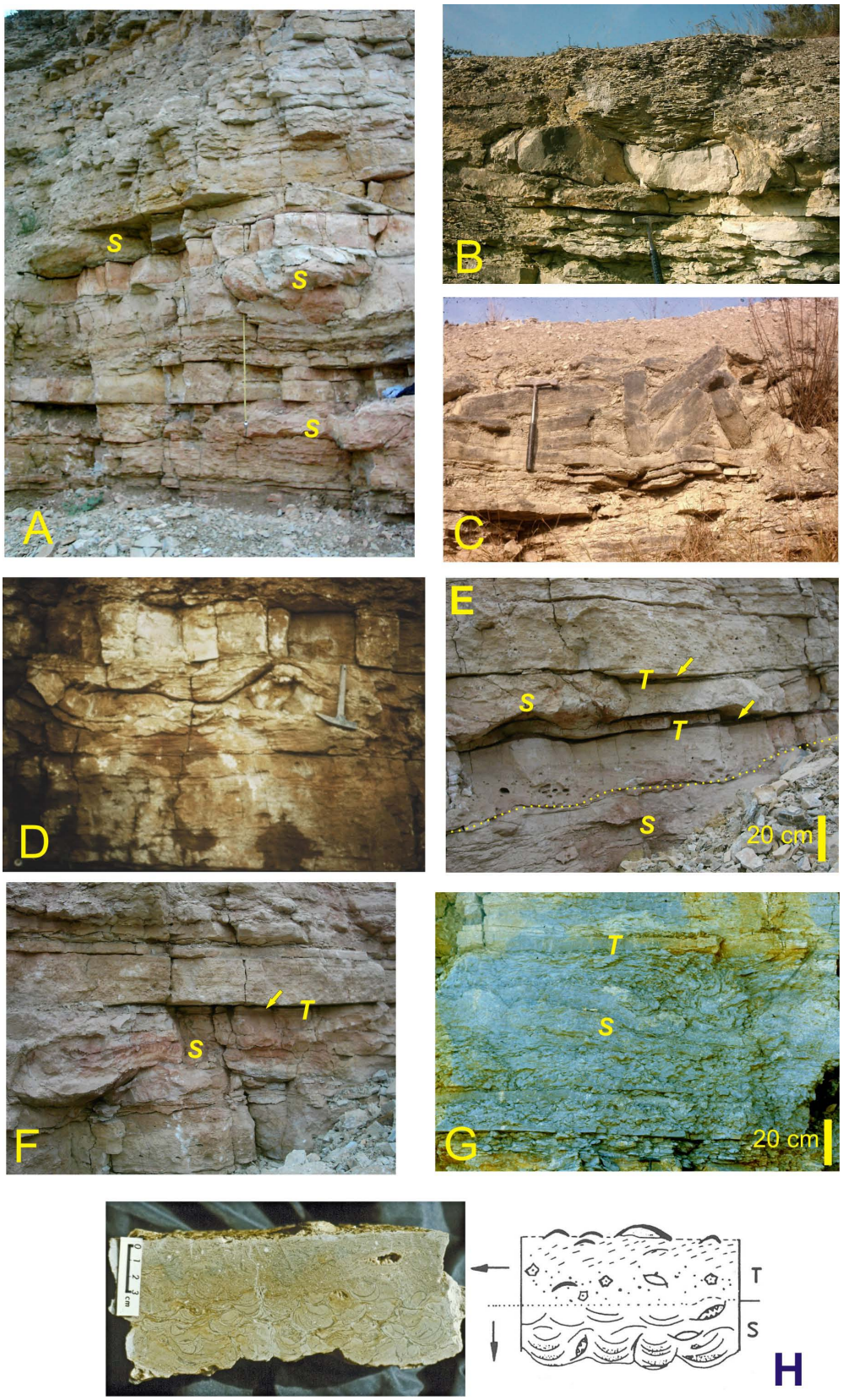

Fig. 13. Sedimentary deformations related to Triassic synsedimentary tectonic activity in southern Poland. **A** – Three, quake-triggered, debris flows (s) in Lower Gogolin Beds. Żyglin, **B-C** – Quake-triggered debris flows in Lower Gogolin Beds. Gogolin, **D** – Quake-triggered deformations in Lower Gogolin Beds. Płaza, **E-F** – Seismite-tsunamite dyads in Lower Gogolin Beds, from Żyglin. S – seismically disturbed sediments (seismite), T – tsunami backflow deposits (tsunamite) composed of offshore-derived intraclastic sediment and land-derived red clayey drape (arrows), **G** – Seismite-tsunamite dyad from Terebratula Beds. Strzelce Opolskie quarry. S – quake-induced slump of lime muds, T – tsunami backflow coquinas bed, **H** – Photograph and drawing of quake-generated bipartite coquina bed from Terebratula Beds. S – convex-down disposed *Coenothyris vulgaris* shells (seismite), unidirectionaly transported skeletal debris (tsunamite). Arrows indicate sense of deplacement.

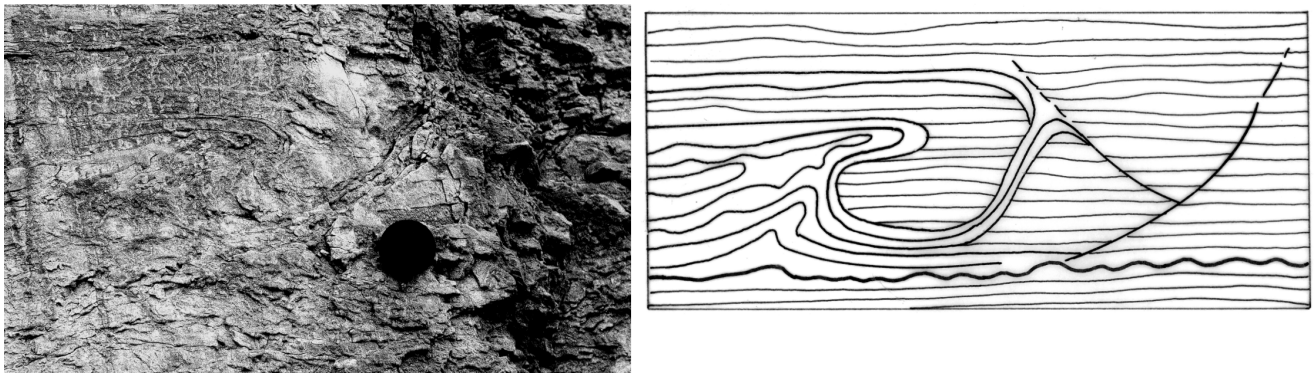

Fig. 14. Photograph and drawing of complex fault-and-fold deformations developed in lime muds affected by seismic shock. Terebratula Beds. Strzelce Opolskie quarry.

B5.1 Płaza. Active quarry of "Kans-Pol" Płaza

The quarry is situated by the railway station "Płaza", some 2 km NW from the village centre. (50°10′55″ N; 19°43′95″ E)

Leaders: Michał Matysik, Joachim Szulc

The ca. 40 meters thick profile begins with the Upper Röt carbonates, which encompass dolomitic rocks displaying many indicators of extremely shallow environment (coastal sabkha) such as stromatolites, tepee structures, desiccation cracks and postevaporitic silicification. The fauna is limited to linguloids and vertebrate bones and fish scales.

The sabkha sediments are passing upwards into hummocky cross-stratified limestones containing more open-marine fauna i.e. *Myophoria vulgaris* and gastropods. Higher up, the first dadocrinids appear indicating stenohaline, normal marine conditions. This part of the section comprises 3 slumped horizons (Fig. 13D), which could be used as excellent stratigraphic correlation tool with the equivalent sections at Gogolin (stop B5.4) and Żyglin (stop B5.3). The *Placunopsis*-encrusted hardground occurring in this complex, marks the MFS of the An1 depositional sequence. The sequence finishes with vuggy dolomites marking a significant sea-level drop. The subsequent conglomeratic and wavy limestones alternated with tempestites (Upper Gogolin Beds) represent the TST deposits.

The relatively deep-water facies grade into calcarenites and calcisiltites of the Górażdże Beds. These sediments representing the HST deposits terminate the presented profile.

B5.2 Siewierz. "GZD" active quarry

(50°49′83″ N; 19°21′35″ E)

Leaders: Michał Matysik, Joachim Szulc

The site is situated close to the ancestral Kraków-Lubliniec-Hamburg master fault zone (Fig, 2) active also in Middle Triassic. The basement rocks cropping out in the quarry are built of black Devonian (Givetian) dolostones that underwent subaerial weathering and karstification before the Muschelkalk transgression. In the middle of the outcrop, the Devonian basement rocks form a cliff-edged elongate horst. During the Muschelkalk transgression the horst was a fault-bounded island, some 200 m wide and 30–50 meters high, overlapped gradually by Triassic deposits. The island is one of the tectonically controlled horsts, forming a palaeoarchipelago in the Muschelkalk sea (Szulc, 1991). The outcrop abounds in records indicative of tectonic and, in particular, palaeoseismic activity in Triassic time.

The Devonian basement rocks over there, display cracking veinlets (Fig. 10) originated by hydraulic fracturing of rocks (Masson, 1972). Since the cracks were filled with unlithified Muschelkalk material they date the seismic events as Anisian in age.

The frontal, marine/land setting of the fault-bounded island has a profound bearing on seismic activity in the region. Water provided lubricant medium that enhanced fault breaking on the one hand and acted as blasting material (hydraulic fracturing) by its injection into the seismically opened cracks on the other hand.

The Devonian rocks, and sporadically the Muschelkalk limestones, are cut by subvertical calcitic veins. The veins

are 1 to 50 cm wide and are filled with several generations of calcite lining (Figs 10D–F). The veins strike generally NNW–SSE and apparently follow the dominant direction of the master fault. According to stable isotope data, the calcite precipitated from hydrothermal solutions that were most likely discharged by quake-pumping mechanism (Sibson, 1987)

Of particular interest are breccias composed of Devonian clasts fallen to the Triassic unlithified sediments. The falling blocks (up to 10 m across in size) deformed the underlying Muschelkalk sediments (Fig. 10A, 10G). As indicates the rockfall debris deposited as fault-scarp screes, several major quakes wreaked havoc with the island coasts.

An intrafomational disconformity separating two Muschelkalk sequences is another evidence of synsedimentary tilting in the region (Fig. 10H). It is very probable that also very rapid vertical changes between subtidal and supratidal facies, common in the Diplopora Beds, resulted from spasmodic vertical displacements (*yo-yo tectonics*), typical for tectonically active regions (see e.g. Plafker, 1972)

Another indicator of synsedimentary seismic activity are small-scale deformations affecting the fine-grained Muschelkalk deposits and particularly well preserved in microbial mats. There are both small brittle deformations like joints, faults and slicked-sided cracks. They are commonly accompanied by soft-sediment deformation structures: small-scale intraformational folding and liquefaction (Fig. 11I) what indicates their seismic origin.

B5.3 Żyglin – small active quarry

Three small quarries are situated on the left side of a local road heading eastward from the village centre, (nearby church) to the forest (about 1.5 km). (50°48′08″N; 18°96′61″ E)

Leader: Joachim Szulc

The outcrop exposes the Lower Gogolin Beds and enables their comparison with their counterparts in the other presented sections, in Gogolin (ca. 50 km to W) and in Plaza (ca. 40 km to SE). In spite of some subordinate differences, all the sections display close similarity in general lithofacies and biota successions. Also the quake-triggered deformational horizons are recognizable in the mentioned section, thus enhancing the reliability of their correlation (Fig. 13A, E–F).

The presented section comprises two lithofacies assemblages which reflect the progressing earliest Anisian transgression. The lower assemblage encompasses the bioclastic, calcarenitic limestones (Myophoria- and Pecten and Dadorinus Beds) displaying features of proximal tempestites. Upsection, the bioclastic, calcareous sands are replaced by calcilutites with finer-grained tempestitic layers, typical for advanced TST.

These limestones are, in turn, followed by dolomitic marls terminating with cellular limestones. The cellular limestones mark an emersion event identifiable over the entire Silesian subbasin.

However, the most important correlation tool are three contorted horizons which affect the lower part of the presented section. These up to 1 m thick deformed beds may be easily correlated with their counterparts in the Gogolin and Plaza sections. These horizons are of particular interest because their internal composition informs about the sequel phenomena of the seismic tremors. As a rule, a deformed horizon commences with plastically deformed set covered with erosionally overlying gravity-flow sediments (Fig. 13E–F). The last mentioned are mostly twofold: the lower part comprises skeletal debris of offshore fauna whereas the upper one is formed by reddish, kaolinitic clays. Such a sequence may be unequivocally related to seismic-tsunami succession, where the deformed lower part represents the seismite *s.s.* while the overlying offshore-derived sediments have been transported by surge, tsunami back flow.

B5.4 Gogolin – abandoned quarry

The outcrop is situated at the eastern end of the communal waste depot in Gogolin, some 1.5 km from the village centre. (50°50′29″ N; 18°03′09″ E)

Leader: Joachim Szulc

The section presents transgressive succession from evaporitic Röt sediments to normal marine limestones of the Lower Muchelkalk.

The Röt is represented by reddish and ochre-coloured limestones and dolomites, comprising molds after gypsum and halite evaporites. Hopper halite crystals, displacive and reworked gypsum crystals and lack of fauna (but rare bones) as well as chertified stromatolites

(Bodzioch and Kwiatkowski, 1992) indicate very shallow, coastal sabkha environments. Meteoric water influxes and emersion events are evidenced by a quartzose conglomerate horizon and solution breccias which mark the boundary of the 1st Anisian sequence.

The sabkha evaporites are succeeded by more and more open marine carbonates as evidenced by increasing faunal quantity and diversity. The transgression climaxed with bioclastic thick-bedded, cross-stratified limestones with stenohaline dadocrinids (so called Beds with Pecten and Dadocrinus).

The following HST is formed by tempestitic shelly limestones and marls which grade uspection to evaporitic dolomites.

The section affords excellent structures related to synsedimentary seismic activity; faults, joints, liquefaction and three debris flows with deplaced slabs reaching 4 meters in size (Fig. 13B–C). The latter are equivalents of those presented at Płaza and Żyglin.

B5.5 Tarnów Opolski. Active quarry of Opolwap – Lhoist

Entrance to the vast quarry (some 10 km^2) is situated 400 m east from the railway station Tarnów Opolski. (50°55′29″ N; 18°08′51″ E)

Leaders: Hans Hagdorn, Michał Matysik, Joachim Szulc

The quarry exposes the uppermost part of the Terebratula Beds and the complete section of the Karchowice Beds.

The deeper-water, fine-grained limestones and marls of the Terebratula Beds evolve gradually into massive, bioclastic Karchowice Beds by 4 meters-thick set of firmgrounds alternated with tempestitic encrinites. The bioclastic sands form locally several meters high dunes, composed of amalgamated cross-stratified sandbodies.

Biolithic complex which developed upwards is dominated by sponge constructions; biostromes, and higher up, by bioherms. The latter reach up to 7 m in height and several tens of meter in width. The other contributors of the bioherms are encrusting worms and forams, crinoids, brachiopods, gastropods and scleractinian corals (Figs. 6–9). The corals are represented by some 20 species which makes this assemblage the oldest (and richest) known scleractinian coral colonies at all (Morycowa, 1988).

The biohermal complex of the Karchowice Beds is bipartite. In the lower part, between the hexactinellid sponges, the colonies of denroid-phaceoloid *Volzeia szulci* occur (Fig. 9c). Delicate branching coral habits, suggest a relatively quiet environment. The corals and sponges form knobs clustered together. This complex is capped by a crust of lamellar colonies of *Pamiroseris silesiaca* (Fig. 9b). Encrusting form of the coral colonies is typical for turbulent environment and indicates that the reef structures reached its shallowest growth phase. The crests of the lower biohermal complex were partly emerged and underwent meteoric diagenesis (dolomitisation, karstfication), while the in local depressions the *Girvanella* oncoliths formed. The bioherms are composed mainly of relatively homogenous, massive or nodular micritic fabrics, which represent aggregates of automicritic carbonate originated by microbially mediated decay of the sponge bodies.

During the next transgressive pulse, the second biohermal complex formed. Its structural framework is similar like in the lower one, but the branching corals are absent.

Total thickness of the biohermal complexes in the reef-core area reaches up to 25 meters.

Vertical succession in the buildup composition reflects ecological evolution related to a highstand shallowing trend, typical of the "catch-up reef" *sensu* James & Mcintyre (1985). As a rule, the succession begins with biostromes built by prostrate colonies of sponges (stabilization-colonisation stage) The biostromes are replaced, first by low-relief, and then by high-relief biohermal buildups, encompassing also branching corals and clusters of other organisms (diversification stage). The reef cap formed by encrusting corals is typical for the final, domination stage of the reef evolution.

The eventual shallowing resulted in decline of the sponge-coral association which has been replaced by oncolithic and oolitic limestones of the Diplopora Beds.

It is worthy to note that the Karchowice Beds display intense lateral variation both on a bed level and within the entire unit. Such a variation challenges the merit of the cyclostratigraphical interpretations for the higher frequency, 4th and 5th orders, depositional sequences.

B5.6 Strzelce Opolskie. Active quarry of Heidelberg Cement GmbH

The huge quarry is situated 1 km east from the local road Strzelce Opolskie- Rozmierka. (50°53′20″ N; 18°30′93″E)

Leaders: Michał Matysik, Joachim Szulc

The section exposes the most complete Lower Muschelkalk outcrop encompassing sediments of two Anisian depositional sequences; A2 and A3 (Fig. 5).

The exposed section commences with marls and distal calcareous tempestites representing maximum flooding zone of the sequence A2, which is concurrent with beginning of the Pelsonian stage. First appearance of the index conodonts, ammonoids and crinoids is the most important bioevent recorded in this interval, indicating open communication with the Tethys.

The subsequent thick-bedded and coarse-grained bioclastic, oncoidal and oolitic limestones build a 15 m thick shoalbar set of the Górazdże Beds. The Gorażdże Beds, which represent HST of the A2 sequence, are built by alternated calcarenites and finer-grained limestones. The calcarenites are cross-stratified, amalgamated oscillatory ripples, transported and deposited under storm wave and current action. The interbedded, fine-grained limestones are fair-weather sediments are intensively bioturbated, which resulted in their nodular character. It is worthy to note, that the oncoids are built mostly by foraminiferal aggregates. The other bioclasts comprise debris of gastropods, pelecypods, crinoids, corals and sponge spicules.

Oomoldic porosity and ferricrete crust featuring the topmost part of the Gorażdze Beds indicate meteoric influences as the shoalbar became emerged (Szulc, 1999). Therefore, one may accept the top of the Gorażdze Beds as a boundary of the next depositional sequence.

This sequence boundary is covered sharply by dark, finely laminated limestones, typical for TST, beginning the Terebratula Beds. These calcilutites are impoverished in body- and ichnofossils, which indicates very fast advancement of the transgression and poorly ventilated, starving basin conditions. This horizon (ca. 1.5–2 m thick) is slumped and totally contorted (Fig. 11M), which suggests a quake-triggered mechanism of the deplacement on the one hand, and tectonically forced deepening on the other hand (Szulc, 1993).

The slumped set is replaced by a 1.5 thick, amalgamated encrinitic bank (so called *Hauptcrinoidenbank* of Assmann, 1944) indicating some shallowing trend. The *Hauptcrinoidenbank* is covered by a 12 meters thick set of slightly dysoxic, grey marls intercalated with dm-thick coquinas, dominated by *Coenothyris vulgaris* shell debris. The Terebratula Beds represent the Anisian maximum flooding interval, recognized over the whole Germanic Basin (Szulc, 1990; Aigner and Bachmann, 1992). Total thickness of the Terebratula Beds reaches ca. 20 meters in the quarry.

The Terebratula Beds are followed by bioclastic (mostly crinoidal) calcarenites alternated with firmground horizons and then by spongean structures forming the Karchowice Beds.

Acknowledgements: This field-trip guidebook is partly based on guidebooks prepared on the occasion of some former conferences, particularly, 6th Annual Conference of SEPM-CES Field Guide (Szulc *et al*., 2009) and Fieldtrip Guide of 4th Meeting on Pan-European Correlation of the Epicontinental Triassic (Szulc *et al*., 2007).

References

Ahlburg, J., 1906. Die Trias im südlichen Oberschlesien. *Abhandlungen der königlich-preußischen geologischen Landesanstalt N. F.*, 50: 1–163.

Aigner, T. & Bachmann, G., 1992 . Sequence-stratigraphic framework of the German Triassic. *Sedimentary Geology,* 80: 115–135.

Alexandrowicz, S. & Siedlecki, S., 1960. Bunter deposits in the vicinity of Rybnik, Upper Silesia. *Rocznik Polskiego Towarzystwa Geologicznego*, 30: 167–199. [in Polish, English summary.]

Assmann, P., 1913. Beitrag zur Kenntnis der Stratigraphie des oberschlesischen Muschelkalks. *Jahrbuch der königlich preußischen geologischen Landesanstalt*, 34: 268–340.

Assmann, P., 1915. Die Brachiopoden und Lamellibranchiaten der oberschlesischen Trias. *Jahrbuch der königlich preußischen geologischen Landesanstalt,* 36: 586-683.

Assmann, P., 1924. Die Gastropoden der oberschlesischen

Trias. *Jahrbuch der preußischen geologischen Landesanstalt,* 44: 1–50.

Assmann, P., 1925. Die Fauna der Wirbellosen und die Diploporen der oberschlesischen Trias mit Ausnahme der Brachiopoden, Lamellibranchiaten, Gastropoden und Korallen. *Jahrbuch der preußischen geologischen Landesanstalt,* 46: 504–577

Assmann, P., 1927. Die Decapodenkrebse des deustchen Muschelkalks. *Jahrbuch der preußischen geologischen Landesanstalt,* 48: 332–356.

Assmann, P., 1937. Revision der Fauna de Wirbellosen der oberschlesischen Trias. *Abhandlungen. der preußischen geologischen Landesanstalt N. F.*, 170: 1–134.

Assmann, P., 1944. Die Stratigraphie der oberschlesischen Trias. Teil 2: Der Muschelkalk. *Abhandlungen. des Reichsamts für Bodenforschung*, 2: 1–124.

Beutler G., 2005. Diskordanzen im Keuper. In: *Stratigpraphie von Deutschland IV – Keuper, Courier Forschungsinstitut Senckenberg*, 253: 85–93.

Bodzioch, A. & Kwiatkowski, S., 1992. Sedimentation and early diagenesis of Cavernous Limestone (Roet) of Gogolin, Silesian-Kraków Upland. *Annales Societatis Geologorum Poloniae,* 62: 223–254.

Brack, P., Rieber, H. & Ulrichs, M., 1999. Pelagic successions in the Southern Alps and their correlation with the Germanic Middle Triassic. *Zentralblatt für Geologie und Paläontologie* Teil I, 1998 (7–8): 813–852.

Dunker, W., 1851. Ueber die im Muschelkalk von Oberschlesien bis jetzt gefundenen Mollusken. *Palaeontographica,* 1: 283–310.

Eck, H., 1865. *Ueber die Formationen des bunten Sandsteins und des Muschelkalks in Oberschlesien und ihre Versteinerungen*. Berlin, Friedländer u. Sohn, 149 pp.

Götz, E. E., Szulc, J. & Feist-Burkhardt, S., 2005. Distribution of sedimentary organic matter in Anisian carbonate series of S Poland: evidence of third-order sea-level fluctuations. *International Journal of Earth Sciences*, 94: 267–274.

Hagdorn, H., 1991. The Muschelkalk in Germany – An Introduction. In: Hagdorn, H., Simon, T. & Szulc, J. (eds), *Muschelkalk. A Field Guide*. Goldschneck-Verlag. Stuttgart, 80 pp.

Hagdorn, H. & Głuchowski, E., 1993. Paleobiogeography and Stratigraphy of Muschelkalk Echinoderms (Crinoidea, Echinoidea) in Upper Silesia. In: Hagdorn, H. & Seilacher, A. (eds), *Muschelkalk*. Goldschneck V. Stuttgart: 165–176.

James, N. P. & Mcintyre J. G., 1985. Carbonate depositional environments, modern and ancient. *Quaterly Journal of the Colorado School of Mines*, 80: 1–70.

Kotański, Z., 1994. Middle Triassic Dasycladacea of the Upper Silesian-Cracow region and their stratigraphical and palaeoecological significance. In: *3rd International Meeting of Peri-Tethyan Epicratonic Basins*, *Cracow, 29 August–3 September 1994. Excursion Guidebook*. PIG Warsaw, pp. 59–66.

Kozur, H., 1974. Probleme der Triasgliederung und Parallerisierung der germanischen und tethyalen Trias. Teil I: Abgrenzung und Gliederung der Trias. *Freiberger Forschungshefte*, C 298: 139–198.

Masson, H., 1972. Sur lorigine de la cornieule par fracturation hydraulique. *Eclogae Geologicae Helvetiae*, 65: 27-41.

Matysik, M., 2014. Sedimentology of the „ore-bearing dolomite" of the Kraków-Silesia region (Middle Triassic, southern Poland). *Annales Societatis Geologorum Poloniae*, 84: 81–112.

Matysik, M., 2015 (in press). Facies types and depositional environments of a morphologically diverse carbonate platform: a case study from the Muschelkalk (Middle Triassic) of Upper Silesia, southern Poland. *Annales Societatis Geologorum Poloniae*.

Meyer, H. von, 1849. Fische, Crustaceen, Echinodermen und andere Versteinerungen aus dem Muschelkalk Oberschlesiens. *Palaeontographica*, 1 (5): 216–242, (6): 243–279

Morycowa, E., 1988. Middle Triassic Scleractinia from the Cracow-Silesia region, Poland. *Acta Paleontologica Polonica*, 33: 91–121.

Narkiewicz, K. & Szulc, J. 2004. Controls of migration of conodont fauna in peripheral oceanic areas. An example from the Middle Triassic of the Northern Peri-Tethys. *Géobios*, 37: 425–436.

Nawrocki, J. & Szulc, J., 2000. The Middle Triassic magnetostratigraphy from the Peri-Tethys basin in Poland. *Earth and Planetary Science Letters,* 182: 77–92.

Plafker, G., 1972. Alaskan earthquake of 1964 and Chilean earthquake of 1960: implications for arc tectonics. *Journal of Geophysical Research*, 77: 901–924.

Rüffer, T., 1996. Seismite im Unteren Muschelkalk westlich von Halle. *Hallesches Jahrbuch fuer Geowissenschaften,* 18: 119–130.

Seilacher, A., 1969. Fault-graded beds interpreted as seis-

mites. *Sedimentology*, 17: 155–159.

Sibson, R. H., 1987. Earthquake rupturing as a mineralizing agent in hydrothermal systems, *Geology*, 15: 701–704.

Schüller, F., Beutler, G & Frantzke, H. J., 1989. Über synsedimentäre Bruchtektonik an der Grenze Unterer/Mittlerer Buntsandstein auf der Hermundurischen Scholle. *Hallesches Jahrbuch für Geowissenschaften*, 14: 49–54.

Schwarz, H.-U., 1970. *Zur Sedimentologie und Fazies des Unteren Muschelkalkes in Südwestdeutschland und angrenzenden Gebieten.* PhD Diss. of the Tübingen University: 297 pp.

Szulc, J., 1990. Diagenesis. IAS International Workshop – Field Seminar. In: *The Muschelkalk – Sedimentary Environments, Facies and Diagenesis. Cracow – Opole. Excursion Guidebook and Abstracts*: pp. 26–28.

Szulc, J., 1991. The Upper Silesian Muschelkalk – a general setting. In: Hagdorn, H., Simon, T. & Szulc, J. (eds), *Muschelkalk. A Field Guide*. Goldschneck V., Stuttgart, pp. 61–63.

Szulc, J., 1993. Early Alpine Tectonics and Lithofacies Succession in the Silesian Part of the Muschelkalk Basin. A Synopsis. In: Hagdorn, H. and Seilacher A., (eds), *Muschelkalk*. Goldschneck V. Stuttgart : 19-28.

Szulc, J., 1995. Schemat stratygrafii sekwencyjnej epikontynentalnego triasu; rola tektoniki i eustatyki. In: *IV Krajowe Spotkanie Sedymentologów P.T.G.*, Kraków, pp. 112–113 [in Polish.]

Szulc, J., 1999. Anisian-Carnian evolution of the Germanic basin and its eustatic, tectonic and climatic controls. *In*: Bachmann, G. H. & Lerche, I. (eds), Epicontinental Triassic. *Zentralblatt für Geologie und Paläontologie, Teil I*, 1998, 7-8: 813–852

Szulc, J., 2000., Middle Triassic evolution of the nortnern Peri-Tethys as influenced by early opening of the Tethys Ocean. *Annales Societatis Geologorum Poloniae*, 70: 1–48.

Szulc, J., 2005. Sedimentary environments of the vertebrate-bearing Norian deposits from Krasiejow, Upper Silesia (Poland). *Hallesches Jahrbuch für Geowissenschaften, Reihe B*, 19: 161-170.

Szulc , J., Gradzinski, M., Lewandowska, A. & Heunisch, C. 2006. The Upper Triassic crenogenic limestones in Upper Silesia (southern Poland) and their paleoenvironmental context. In: Alonso-Zarza, A. & Tanner, L. H. (eds), *Paleoenvironmental Record and Applications of Calcretes and Palustrine Carbonates*. Geological Society of America Special Paper, 416: 133-151.

Trammer, J., 1975. Stratigraphy and facies development of the Muschelkalk in the south-western Holy Cross Mts. *Acta Geologica Polonica,* 25: 179–216.

Voigt, T. & Linnemann, U., 1996. Resedimentation im Unteren Muschelkalk- das Profil am Jenzig bei Jena. *Beitraege zur Geologie Thüringen*, *N.F.*, 3: 153–167.

Zawidzka, K., 1975. Conodont stratigraphy and sedimentary environment of the Muschelkalk in Upper Silesia. *Acta Geologica Polonica,* 25: 217–257.

The Organizing Committee would like to acknowledge the generous support of our Sponsors, Patrons, Partners and Exhibitors

Ministry of Science and Higher Education
Republic of Poland

Platinum Sponsor

ORLEN Upstream

Silver Partner

PGNiG
Polish Oil & Gas Company

Silver Sponsor

Springer

Patron

WIELICZKA SALT MINE

USB Flash-Drive Sponsor

WILEY

Writing-Pad & Writing-Pen Sponsor

SHALETECH ENERGY

Patron Sponsor

BETA
Radiocarbon Dating
Consistent Accuracy Delivered On-Time
Beta Analytic Ltd.

CoCaRDE

European Science Foundation

ZGM Bolesław

Muszynianka
naturalna woda mineralna

Lanyard Sponsor

ZEISS

Exhibitors

geokrak

SYL & ANT Instruments

INTROLIGATORNIA
Wiesław Nowotarski


2015
KRAKÓW